DESY 99/171
PM/99-55
TTP99-48
hep-ph/0001169
LC-TH-2000-027

The Reconstruction of Trilinear Higgs Couplings*

A. Djouadi[1], W. Kilian[2], M. Muhlleitner[3] and P.M. Zerwas[3]

[1] *Lab. de Physique Mathématique, Université Montpellier, F-34095 Montpellier Cedex 5*
[2] *Institut für Theoretische Teilchenphysik, Universität Karlsruhe, D-76128 Karlsruhe*
[3] *Deutsches Elektronensynchrotron DESY, D-22603 Hamburg*

Abstract

To establish the Higgs mechanism *sui generis* experimentally, the Higgs self-interaction potential must be reconstructed. This task requires the measurement of the trilinear and quadrilinear self-couplings, as predicted in the Standard Model or in supersymmetric theories. The couplings can be probed in multiple Higgs production at high-luminosity e^+e^- linear colliders. We present the theoretical analysis for the production of neutral Higgs-boson pairs in the relevant channels of double Higgs-strahlung and associated multiple Higgs production.

*Proceedings, *Physics with a High-Luminosity e^+e^- Linear Collider*, DESY/ECFA LC Workshop, DESY 99-123F.

1. Introduction

1. The Higgs mechanism [1] is a cornerstone in the electroweak sector of the Standard Model (SM) [2]. The electroweak gauge bosons and the fundamental matter particles acquire masses through the interaction with a scalar field. The self-interaction of the scalar field leads to a non-zero field strength $v = (\sqrt{2}G_F)^{-1/2} \approx 246$ GeV in the ground state, inducing the spontaneous breaking of the electroweak $\mathrm{SU(2)_L \times U(1)_Y}$ symmetry down to the electromagnetic $\mathrm{U(1)_{EM}}$ symmetry.

To establish the Higgs mechanism *sui generis* experimentally, the characteristic self-energy potential of the Standard Model,

$$V = \lambda \left[|\varphi|^2 - \tfrac{1}{2} v^2 \right]^2 \tag{1}$$

with a minimum at $\langle \varphi \rangle_0 = v/\sqrt{2}$, must be reconstructed once the Higgs particle will be discovered. This experimental task requires the measurement of the trilinear and quadrilinear self-couplings of the Higgs boson. The self-couplings are uniquely determined in the Standard Model by the mass of the Higgs boson which is related to the quadrilinear coupling λ by $M_H = \sqrt{2\lambda} v$. Introducing the physical Higgs field H in the neutral component of the doublet, $\varphi_0 = (v + H)/\sqrt{2}$, the multiple Higgs couplings can be derived from the potential V:

$$V = \frac{M_H^2}{2} H^2 + \frac{M_H^2}{2v} H^3 + \frac{M_H^2}{8v^2} H^4 \tag{2}$$

The trilinear and quadrilinear vertices of the Higgs field H are given by the coefficients:

$$\lambda_{HHH} = 3M_H^2/M_Z^2 \qquad [\text{unit} : \lambda_0 = M_Z^2/v \approx 33.8 GeV] \tag{3}$$

$$\lambda_{HHHH} = 3M_H^2/M_Z^4 \qquad [\text{unit} : \lambda_0^2\,] \tag{4}$$

For a Higgs mass $M_H = 110$ GeV, the trilinear coupling amounts to $\lambda_{HHH}\lambda_0/M_Z = 1.6$ for a typical energy scale M_Z, whereas the quadrilinear coupling $\lambda_{HHHH}\lambda_0^2 = 0.6$ is suppressed with respect to the trilinear coupling by a factor close to the size of the weak gauge coupling.

The trilinear Higgs self-coupling can be measured directly in pair-production of Higgs particles at hadron and high-energy e^+e^- linear colliders. Several mechanisms that are sensitive to λ_{HHH} can be exploited for this task. Higgs pairs can be produced through double Higgs-strahlung off W or Z bosons [3,4], WW or ZZ fusion [4–8]; moreover through gluon-gluon fusion in pp collisions [9–11] and high-energy $\gamma\gamma$ fusion [4,5,12] at photon colliders. In a precursor to this report [13] it was recently shown that for collider energies up to about 1 TeV double Higgs-strahlung is the most promising process for measuring the trilinear coupling:

$$\text{double Higgs-strahlung:} \quad e^+e^- \xrightarrow[Z]{} ZHH \tag{5}$$

As evident from Fig. 1, the trilinear coupling is involved only in one diagram of this process. However, the two other diagrams are generated by the electroweak gauge interactions, and

double Higgs-strahlung: $e^+e^- \to ZHH$

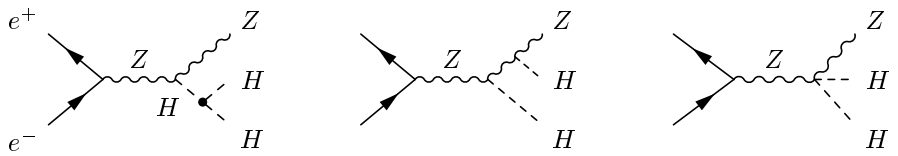

Figure 1: *Subprocesses contributing to double Higgs-strahlung in the Standard Model at e^+e^- linear colliders.*

can thus be assumed known since the Higgs-gauge coupling is measured directly in the basic process of single Higgs-strahlung.

After the decay of the Higgs bosons into b and τ pairs many reducible electroweak and QCD background processes contribute to the final state. It has been demonstrated in careful experimental simulations [14] and phenomenological analyses [15] that the signal can nevertheless be isolated in a clean form.

With values typically of the order of a few fb and below, the cross sections are small at e^+e^- linear colliders for masses of the Higgs boson in the intermediate mass range. High luminosities are therefore needed to produce a sufficiently large sample of Higgs-pair events and to isolate the signal from the background.

2. If a light Higgs boson with a mass below about 130 GeV will be discovered, the Standard Model is likely embedded in a supersymmetric theory. The minimal supersymmetric extension of the Standard Model (MSSM) includes two iso-doublets of Higgs fields φ_1, φ_2 which, after three components are absorbed to provide longitudinal degrees of freedom to the electroweak gauge bosons, gives rise to a quintet of physical Higgs boson states: h, H, A, $H^\pm$ [16]. While an upper bound of about 130 GeV can be derived on the mass of the light CP-even neutral Higgs boson h [17,18], the heavy CP-even and CP-odd neutral Higgs bosons H, A, and the charged Higgs bosons $H^\pm$ may have masses of the order of the electroweak symmetry scale v up to about 1 TeV. This extended Higgs system can be described by two parameters at the tree level: one mass parameter which is generally identified with the pseudoscalar A mass M_A, and $\tan\beta$, the ratio of the vacuum expectation values of the two neutral fields in the two iso-doublets.

The mass parameters and the couplings in the self-interaction potential of the two Higgs doublets are affected by top and stop-loop radiative corrections. Radiative corrections in the one-loop leading M_t^4 approximation are parameterized by

$$\epsilon \approx \frac{3G_F M_t^4}{\sqrt{2}\pi^2 \sin^2\beta} \log\frac{\tilde{M}^2}{M_t^2} \tag{6}$$

where the scale of supersymmetry breaking is characterized by a common squark-mass value

$\tilde{M}$ which will be set to 1 TeV in the numerical analyses; if stop mixing effects are modest at the SUSY scale, they can be accounted for by shifting $\tilde{M}^2$ in ϵ by the amount

$$\begin{aligned} \tilde{M}^2 \to \tilde{M}^2 + \Delta\tilde{M}^2 \quad : \quad \Delta\tilde{M}^2 &= \hat{A}^2[1 - \hat{A}^2/(12\tilde{M}^2)] \\ \hat{A} &= A - \mu \cot\beta \end{aligned} \tag{7}$$

where A and μ correspond to the trilinear coupling in the top sector and the higgsino mass parameter in the superpotential, respectively. The neutral CP-even Higgs boson masses, and the mixing angle α in the neutral sector are given in this approximation by

$$\begin{aligned} M^2_{h,H} &= \tfrac{1}{2}\left[M_A^2 + M_Z^2 + \epsilon \mp \sqrt{(M_A^2 + M_Z^2 + \epsilon)^2 - 4M_A^2 M_Z^2 \cos^2 2\beta - 4\epsilon(M_A^2 \sin^2\beta + M_Z^2 \cos^2\beta)}\right] \\ \tan 2\alpha &= \tan 2\beta \frac{M_A^2 + M_Z^2}{M_A^2 - M_Z^2 + \epsilon/\cos 2\beta} \qquad \text{with} \qquad -\frac{\pi}{2} \leq \alpha \leq 0 \end{aligned} \tag{8}$$

when expressed in terms of the mass M_A and $\tan\beta$.

The set of trilinear couplings between the neutral physical Higgs bosons can be written [17,19] in units of λ_0 as

$$\begin{aligned} \lambda_{hhh} &= 3\cos 2\alpha \sin(\beta+\alpha) + 3\frac{\epsilon}{M_Z^2}\frac{\cos\alpha}{\sin\beta}\cos^2\alpha \\ \lambda_{Hhh} &= 2\sin 2\alpha \sin(\beta+\alpha) - \cos 2\alpha \cos(\beta+\alpha) + 3\frac{\epsilon}{M_Z^2}\frac{\sin\alpha}{\sin\beta}\cos^2\alpha \\ \lambda_{HHh} &= -2\sin 2\alpha \cos(\beta+\alpha) - \cos 2\alpha \sin(\beta+\alpha) + 3\frac{\epsilon}{M_Z^2}\frac{\cos\alpha}{\sin\beta}\sin^2\alpha \\ \lambda_{HHH} &= 3\cos 2\alpha \cos(\beta+\alpha) + 3\frac{\epsilon}{M_Z^2}\frac{\sin\alpha}{\sin\beta}\sin^2\alpha \\ \lambda_{hAA} &= \cos 2\beta \sin(\beta+\alpha) + \frac{\epsilon}{M_Z^2}\frac{\cos\alpha}{\sin\beta}\cos^2\beta \\ \lambda_{HAA} &= -\cos 2\beta \cos(\beta+\alpha) + \frac{\epsilon}{M_Z^2}\frac{\sin\alpha}{\sin\beta}\cos^2\beta \end{aligned} \tag{9}$$

In the decoupling limit $M_A^2 \sim M_H^2 \sim M_{H^\pm}^2 \gg v^2/2$, the self-coupling of the light CP-even neutral Higgs boson h approaches the SM value.

In the subsequent numerical analysis the complete one-loop and the leading two-loop corrections to the MSSM Higgs masses and to the trilinear couplings are included, as presented in Ref. [18,20]. Mixing effects due to non-vanishing A, μ parameters primarily affect the light Higgs mass; the upper limit on M_h depends strongly on the size of the mixing parameters, raising this value for $\tan\beta \gtrsim 2.5$ beyond the reach of LEP2, cf. Ref. [21]. The couplings however are affected less by higher-order corrections when evaluated for the physical Higgs masses. The variation of the trilinear couplings with M_A is shown for two values $\tan\beta = 3$ and 50 in Figs. 2a and 2b. The region in which the couplings vary rapidly, corresponds to the h/H cross-over region of the two mass branches in the neutral CP-even sector, cf. eq. (8). The trilinear couplings between h, H and the pseudoscalar pair AA are in general significantly

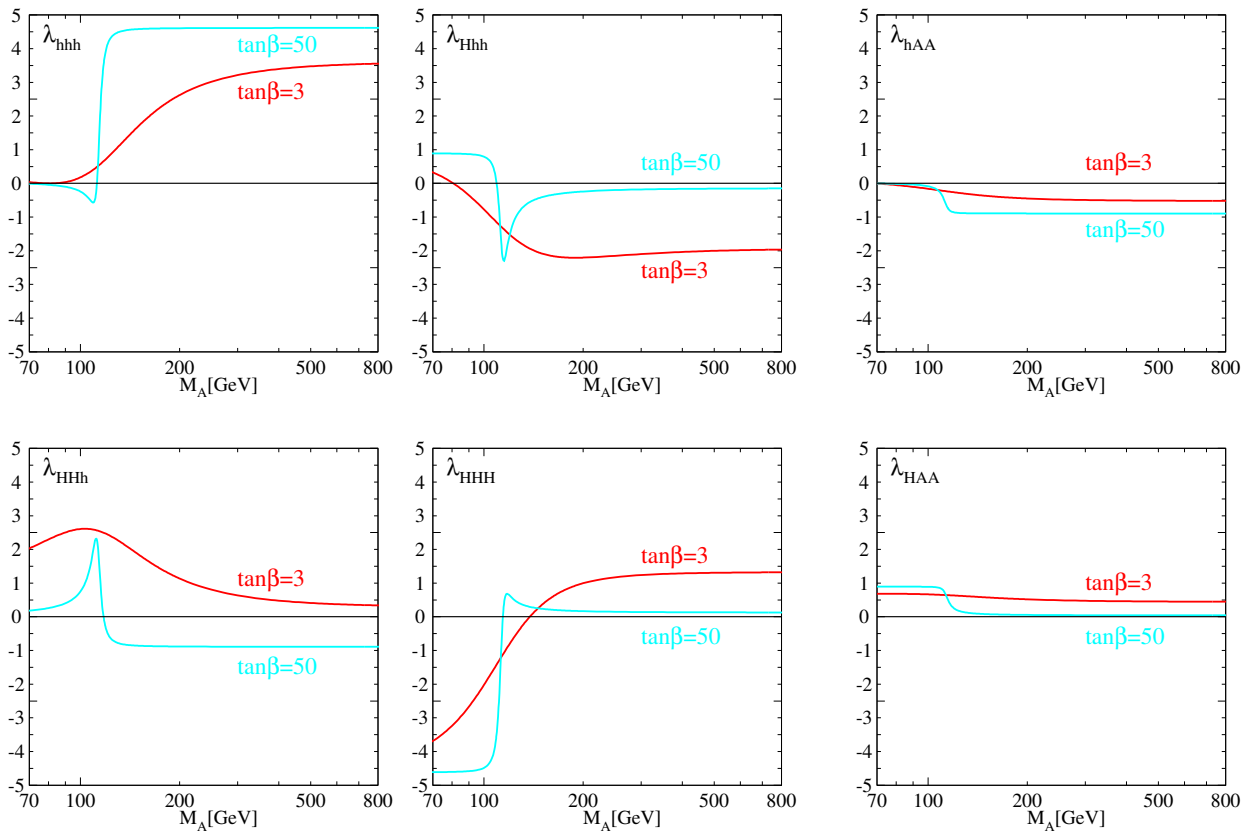

Figure 2a: *Variation of the trilinear couplings with M_A for tanβ = 3 and 50 in the MSSM; the region of rapid variations corresponds to the h/H cross-over region in the CP-even sector.*

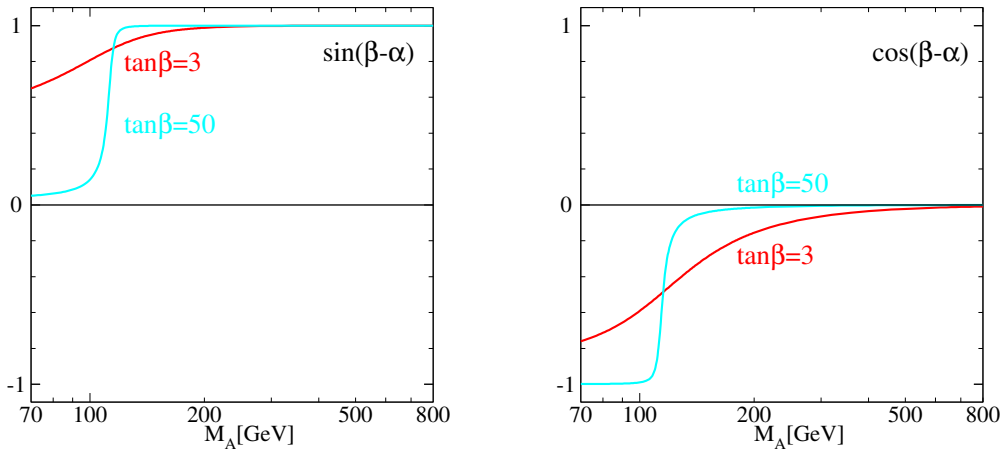

Figure 2b: *ZZh and ZZH gauge couplings in units of the SM coupling.*

	double Higgs−strahlung				triple Higgs−production			
λ	Zhh	ZHh	ZHH	ZAA	Ahh	AHh	AHH	AAA
hhh	×				×			
Hhh	×	×			×	×		
HHh		×	×			×	×	
HHH			×				×	
hAA				×	×	×		×
HAA				×		×	×	×

Table 1: *The trilinear couplings between neutral CP-even and CP-odd MSSM Higgs bosons which can generically be probed in double Higgs-strahlung and associated triple Higgs-production, are marked by a cross. [The matrix for WW fusion is isomorphic to the matrix for Higgs-strahlung.]*

smaller than the trilinear couplings among the CP-even Higgs bosons.

In contrast to the Standard Model, resonance production of the heavy neutral Higgs boson H followed by subsequent decays $H \to hh$, plays a dominant role in part of the parameter space for moderate values of $\tan\beta$ and H masses between 200 and 350 GeV, Ref. [22]. In this range, the branching ratio, derived from the partial width

$$\Gamma[H \to hh] = \frac{\sqrt{2} G_F M_Z^4}{32\pi M_H} \lambda_{Hhh}^2 \beta_h \tag{10}$$

is neither too small nor too close to unity to be measured directly. [The decay of either h or H into a pair of pseudoscalar states, $h/H \to AA$, is kinematically not possible in the parameter range which the present analysis is based upon; if realized, the couplings λ_{hAA} and λ_{HAA} can be determined in the same way.] If double Higgs production is mediated by the resonant production of H, the total production cross section of light Higgs pairs increases by about an order of magnitude [19].

The trilinear Higgs-boson couplings are involved in a large number of processes at e^+e^- linear colliders [19] among which double Higgs-strahlung and triple Higgs production are the preferred channels [13]:

$$\begin{aligned} &\text{double Higgs-strahlung:} \quad e^+e^- \to ZH_iH_j \quad \text{and} \quad ZAA \quad [H_{i,j} = h, H] \\ &\text{triple Higgs production:} \quad e^+e^- \to AH_iH_j \quad \text{and} \quad AAA \end{aligned} \tag{11}$$

The trilinear couplings which enter for various final states, cf. Fig. 3, are marked by a cross in the matrix Table 1. In the ideal case the system could be solved for all λ's, up to discrete

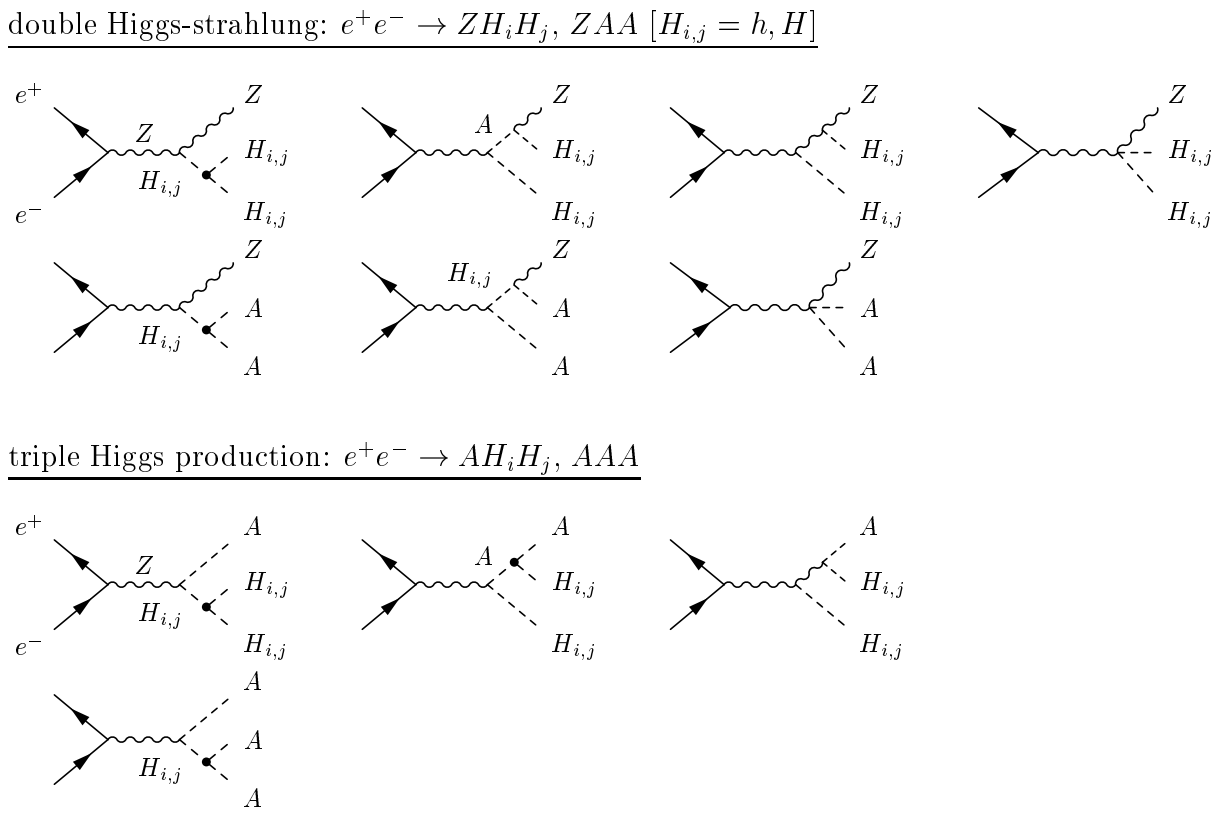

Figure 3: *Processes contributing to double and triple Higgs production involving trilinear couplings in the MSSM.*

ambiguities, based on double Higgs-strahlung, Ahh and triple A production ["bottom-up approach"]. This can easily be inferred from the correlation matrix Table 1. From $\sigma(ZAA)$ and $\sigma(AAA)$ the couplings $\lambda(hAA)$ and $\lambda(HAA)$ can be extracted. In a second step, $\sigma(Zhh)$ and $\sigma(Ahh)$ can be used to solve for $\lambda(hhh)$ and $\lambda(Hhh)$; subsequently, $\sigma(ZHh)$ for $\lambda(HHh)$; and, finally, $\sigma(ZHH)$ for $\lambda(HHH)$. The remaining triple Higgs cross sections $\sigma(AHh)$ and $\sigma(AHH)$ could provide additional redundant information on the trilinear couplings.

In practice, not all the cross sections will be large enough to be accessible experimentally, preventing the straightforward solution for the complete set of couplings. In this situation however the reverse direction can be followed ["top-down approach"]. The trilinear Higgs couplings can stringently be tested by comparing the theoretical predictions of the cross sections with the experimental results for the accessible channels of double and triple Higgs production.

If, as expected in the MSSM, the couplings hAA and HAA are very small, the ZAA and AAA final states can be left out of the analysis. This conclusion can be checked experimen-

tally in a model-independent way, assuming nothing but the knowledge of pre-determined gauge boson-Higgs couplings. The system is then reduced to the trilinear couplings among the CP-even Higgs bosons h, H [in the double-line box of Table 1] which can be measured in the analysis chain outlined in the previous paragraph, based solely on double Higgs-strahlung ZH_iH_j and triple Higgs-production Ahh. The hH_iH_j couplings involving the light Higgs boson h with any combination of CP-even Higgs bosons can thus be determined in total.

The processes $e^+e^- \to ZH_iA$ [$H_i = h, H$] of mixed CP-even/CP-odd Higgs final states are generated through gauge interactions alone, mediated by virtual Z bosons decaying to the CP even–odd Higgs pair, $Z^* \to H_iA$. These parity-mixed processes do not involve trilinear Higgs-boson couplings.

3. In this report we summarize the results of Ref. [13] for the production of Higgs boson pairs in the Standard Model and in the minimal supersymmetric extension. Other aspects have been discussed in Refs. [23,24]. The comparison with LHC channels has been presented in Refs. [25,26]. The analyses have been carried out for e^+e^- linear colliders [27], which are currently designed for an initial phase in the range $\sqrt{s} = 500$ GeV to 1 TeV. The small cross sections require high luminosities as foreseen in the TESLA design with targets of $\int \mathcal{L} = 300$ and 500 fb^{-1} *per annum* for $\sqrt{s} = 500$ and 800 GeV, respectively [28].

The report is divided into two parts. In Section 2 we discuss the measurement of the trilinear Higgs coupling in the Standard Model for double Higgs-strahlung at e^+e^- linear colliders. In Section 3 this program, including the triple Higgs production, is extended to the Minimal Supersymmetric Standard Model MSSM.

2. Higgs Pair–Production in the Standard Model

2.1 Double Higgs-strahlung

The (unpolarized) differential cross section for the process of double Higgs-strahlung $e^+e^- \to ZHH$, cf. Fig. 1, can be cast into the form [19]

$$\frac{d\sigma[e^+e^- \to ZHH]}{dx_1 dx_2} = \frac{\sqrt{2} G_F^3 M_Z^6}{384\pi^3 s} \frac{v_e^2 + a_e^2}{(1-\mu_Z)^2} \mathcal{Z}(x_1, x_2) \tag{12}$$

after the angular dependence is integrated out. The vector and axial-vector Z charges of the electron are defined as usual, by $v_e = -1 + 4\sin^2\theta_W$ and $a_e = -1$. $x_{1,2} = 2E_{1,2}/\sqrt{s}$ are the scaled energies of the two Higgs particles, $x_3 = 2 - x_1 - x_2$ is the scaled energy of the Z boson, and $y_i = 1 - x_i$; the square of the reduced masses is denoted by $\mu_i = M_i^2/s$, and $\mu_{ij} = \mu_i - \mu_j$. In terms of these variables, the coefficient $\mathcal{Z}$ may be written as:

$$\mathcal{Z} = \mathfrak{z}^2 f_0 + \frac{1}{4\mu_Z(y_1 + \mu_{HZ})} \left[\frac{f_1}{y_1 + \mu_{HZ}} + \frac{f_2}{y_2 + \mu_{HZ}} + 2\mu_Z \mathfrak{z} f_3 \right] + \left\{ y_1 \leftrightarrow y_2 \right\} \tag{13}$$

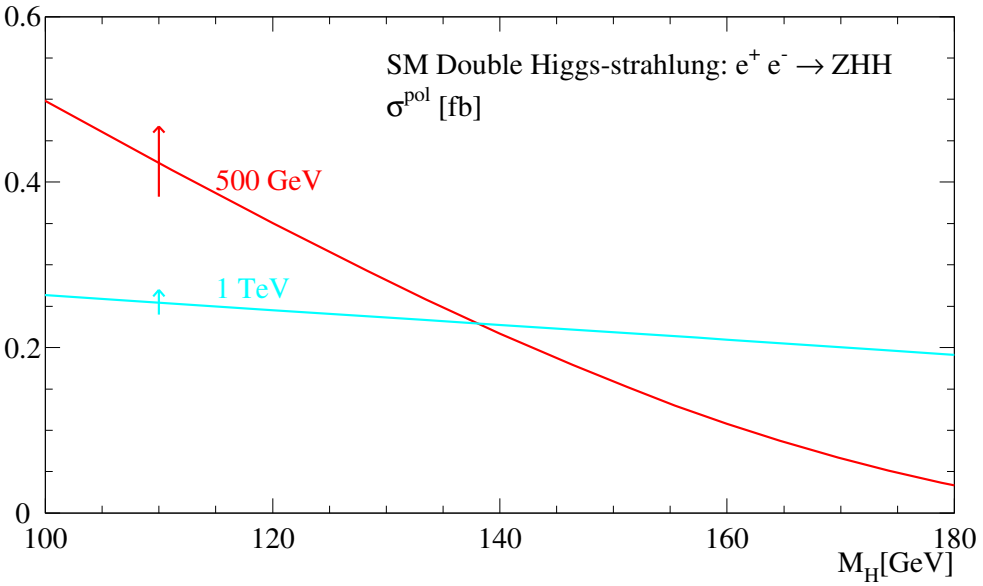

Figure 4a: *The cross section for double Higgs-strahlung in the SM at two collider energies:* 500 *GeV and* 1 *TeV. The electron/positron beams are taken oppositely polarized. The vertical arrows correspond to a variation of the trilinear Higgs coupling from* 0.8 *to* 1.2 *of the SM value.*

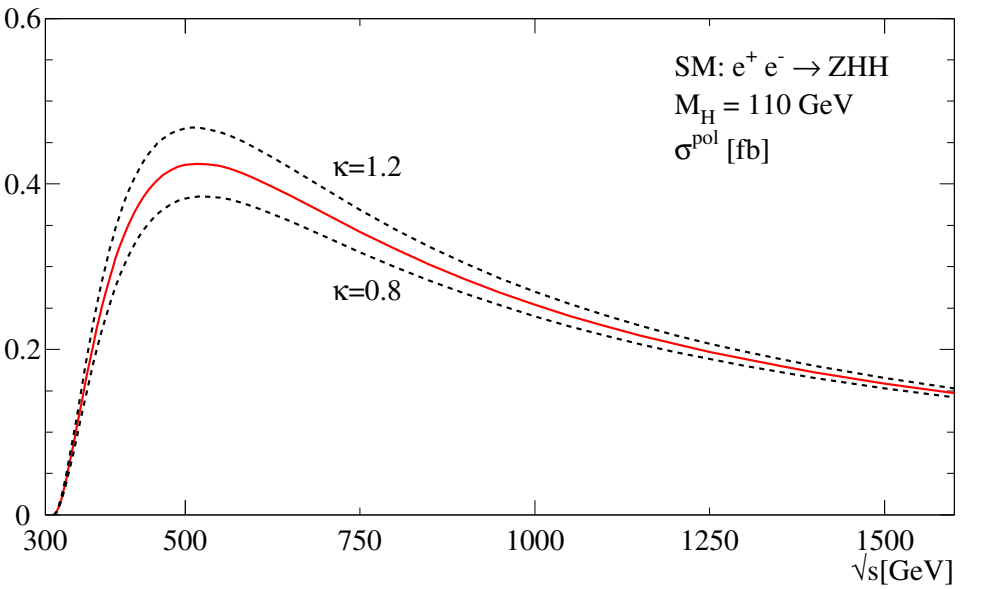

Figure 4b: *The energy dependence of the cross section for double Higgs-strahlung for a fixed Higgs mass* $M_H = 110$ *GeV. The full line corresponds to the trilinear Higgs coupling of the Standard Model. The variation of the cross section for modified trilinear couplings* $\kappa\lambda_{HHH}$ *is indicated by the dashed lines.*

with

$$\mathfrak{z} = \frac{\lambda_{HHH}}{y_3 - \mu_{HZ}} + \frac{2}{y_1 + \mu_{HZ}} + \frac{2}{y_2 + \mu_{HZ}} + \frac{1}{\mu_Z} \tag{14}$$

The coefficients f_i are listed in Ref. [13]. The first term in the coefficient $\mathfrak{z}$ includes the trilinear coupling λ_{HHH}. The other terms are related to sequential Higgs-strahlung amplitudes and the 4-gauge-Higgs boson coupling; the individual terms can easily be identified by examining the characteristic propagators.

Since double Higgs-strahlung is mediated by s-channel Z-boson exchange, the cross section doubles if oppositely polarized electron and positron beams are used.

The cross sections for double Higgs-strahlung in the intermediate mass range are presented in Fig. 4a for total e^+e^- energies of $\sqrt{s} = 500$ GeV and 1 TeV. The cross sections are shown for polarized electrons and positrons, $\lambda_{e^-}\lambda_{e^+} = -1$. As a result of the scaling behavior, the cross section for double Higgs-strahlung decreases with rising energy beyond the threshold region. The cross section increases with rising trilinear self-coupling in the vicinity of the SM value. The sensitivity to the HHH self-coupling is demonstrated in Fig. 4b by varying the trilinear coupling $\kappa\lambda_{HHH}$ within the range $\kappa = 0.8$ and 1.2; the sensitivity is also illustrated by the vertical arrows in Fig. 4a for a variation of κ in the same range. Evidently the cross section $\sigma(e^+e^- \to ZHH)$ is sensitive to the value of the trilinear coupling; the sensitivity is not swamped by the irreducible background diagrams involving only the Higgs-gauge couplings. While the irreducible background diagrams become more important for rising energies, the sensitivity to the trilinear Higgs coupling is very large just above the kinematical threshold for the ZHH final state. Near the threshold the value of the propagator of the intermediate virtual Higgs boson connecting to the two real Higgs bosons through λ_{HHH} in the final state, is maximal. The maximum cross section for double Higgs-strahlung is reached at energies $\sqrt{s} \sim 2M_H + M_Z + 200$ GeV, i.e. for Higgs masses in the lower part of the intermediate range at $\sqrt{s} \sim 500$ GeV.

Below 1 TeV one can always find collider energies at which the cross section for Higgs-strahlung $e^+e^- \to ZHH$ is larger than the cross section for WW fusion of two Higgs bosons, $e^+e^- \to \bar{\nu}_e\nu_e HH$. However, for collider energies above 1 TeV the logarithmic increase of the t-channel fusion process dominates over the Higgs-strahlung mechanism which scales in the energy.

In recent experimental simulations of the Higgs-strahlung process it has been shown that the signal for two-Higgs boson production can be extracted [14] despite the multi-channel reducible background [15]. A sensitivity better than 20% can be expected for the measurement of the trilinear Higgs self-coupling in the lower part of the intermediate Higgs mass range of the Standard Model.

The complete reconstruction of the Higgs potential in the Standard Model requires the

$\sqrt{s} = 1$TeV	$\sigma(e^+e^- \to ZHHH)$[ab]
$M_H = 110$ GeV	0.44 [0.41/0.46]
150 GeV	0.34 [0.32/0.36]
190 GeV	0.19 [0.18/0.20]

Table 2: *Representative values for triple SM Higgs-strahlung (unpolarized beams). The sensitivity to the quadrilinear coupling is illustrated by the variation of the cross sections when* λ_{HHHH} *is altered by factors* $1/2$ *and* $3/2$*, as indicated in the square brackets.*

measurement of the quadrilinear coupling λ_{HHHH}, too. This coupling is suppressed relative to the trilinear coupling by a factor which is effectively of the order of the weak gauge coupling for masses in the lower part of the intermediate Higgs mass range. Access to the quadrilinear coupling can be obtained directly only through the production of three Higgs bosons: $e^+e^- \longrightarrow ZHHH$. However, this cross section is strongly reduced by three orders of magnitude compared to the corresponding double-Higgs channel. As argued before, the signal amplitude involving the four-Higgs coupling [as well as the irreducible Higgs-strahlung amplitudes] is suppressed, leading to a reduction by a factor $[\lambda^2_{HHHH}\lambda_0^4/16\pi^2]/[\lambda^2_{HHH}\lambda_0^2/M_Z^2] \sim 10^{-3}$. Irreducible background diagrams are suppressed by a ratio of similar size. Moreover, the phase space is reduced by the additional heavy particle in the final state. A few illustrative examples of cross sections for triple Higgs-strahlung are listed in Table 2.

3. The Supersymmetric Higgs Sector

A large ensemble of Higgs couplings are present in supersymmetric theories. Even in the minimal realization MSSM, six different trilinear couplings hhh, Hhh, HHh, HHH, hAA, HAA are generated among the neutral particles, and many more quadrilinear couplings. Since in major parts of the MSSM parameter space the Higgs bosons H, A, $H^\pm$ are quite heavy, we will focus primarily on the production of light neutral pairs hh, yet the production of heavy Higgs bosons will also be discussed where appropriate. The channels in which trilinear Higgs couplings can be probed in e^+e^- collisions, have been catalogued in Table 1.

Barring the exceptional case of very light pseudoscalar A states, λ_{Hhh} is the only trilinear coupling that may be measured in resonance decays, $H \to hh$, while all the other couplings must be accessed in continuum pair production. The relevant mechanisms have been categorized in Fig. 3 for double Higgs-strahlung and associated triple Higgs production.

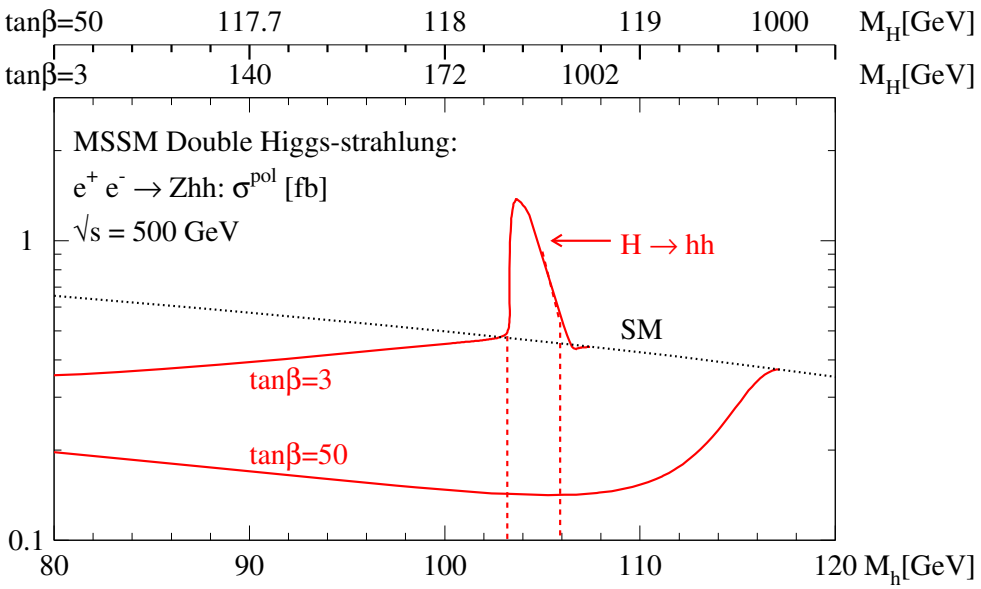

Figure 5: *Total cross sections for MSSM hh production via double Higgs-strahlung at e^+e^- linear colliders for* $\tan\beta = 3,\ 50$ *and* $\sqrt{s} = 500$ GeV, *including mixing effects ($A = 1$ TeV, $\mu = -1/1$ TeV for* $\tan\beta = 3/50$*). The dotted line indicates the SM cross section.*

3.1 Double Higgs-strahlung

The (unpolarized) cross section for double Higgs-strahlung, $e^+e^- \to Zhh$, is modified [13, 19,23] with regard to the Standard Model by H,A exchange diagrams, cf. Fig. 3:

$$\frac{d\sigma[e^+e^- \to Zhh]}{dx_1 dx_2} = \frac{\sqrt{2} G_F^3 M_Z^6}{384\pi^3 s} \frac{v_e^2 + a_e^2}{(1-\mu_Z)^2} \mathcal{Z}_{11}(x_1, x_2) \tag{15}$$

with

$$\begin{aligned} \mathcal{Z}_{11} &= \mathfrak{z}_{11}^2 f_0 + \frac{\mathfrak{z}}{2}\left[\frac{\sin^2(\beta-\alpha) f_3}{y_1+\mu_{1Z}} + \frac{\cos^2(\beta-\alpha) f_3}{y_1+\mu_{1A}}\right] + \frac{\sin^4(\beta-\alpha)}{4\mu_Z(y_1+\mu_{1Z})}\left[\frac{f_1}{y_1+\mu_{1Z}} + \frac{f_2}{y_2+\mu_{1Z}}\right] \\ &+ \frac{\cos^4(\beta-\alpha)}{4\mu_Z(y_1+\mu_{1A})}\left[\frac{f_1}{y_1+\mu_{1A}} + \frac{f_2}{y_2+\mu_{1A}}\right] + \frac{\sin^2 2(\beta-\alpha)}{8\mu_Z(y_1+\mu_{1A})}\left[\frac{f_1}{y_1+\mu_{1Z}} + \frac{f_2}{y_2+\mu_{1Z}}\right] \\ &+ \Big\{y_1 \leftrightarrow y_2\Big\} \end{aligned} \tag{16}$$

and

$$\mathfrak{z}_{11} = \left[\frac{\lambda_{hhh}\sin(\beta-\alpha)}{y_3-\mu_{1Z}} + \frac{\lambda_{Hhh}\cos(\beta-\alpha)}{y_3-\mu_{2Z}}\right] + \frac{2\sin^2(\beta-\alpha)}{y_1+\mu_{1Z}} + \frac{2\sin^2(\beta-\alpha)}{y_2+\mu_{1Z}} + \frac{1}{\mu_Z} \tag{17}$$

The notation follows the Standard Model, with $\mu_1 = M_h^2/s$ and $\mu_2 = M_H^2/s$. In parameter ranges in which the heavy neutral Higgs boson H or the pseudoscalar Higgs boson A becomes resonant, the decay widths are implicitly included by shifting the masses to complex Breit-Wigner values.

The total cross sections are shown in Fig. 5 for the e^+e^- collider energy $\sqrt{s} = 500$ GeV. The parameter $\tan\beta$ is chosen to be 3 and 50, and the mixing parameters $A = 1$ TeV and $\mu = -1$ TeV and 1 TeV, respectively. If $\tan\beta$ and the mass M_h are fixed, the masses of the other heavy Higgs bosons are predicted in the MSSM [22]. Since the vertices are suppressed by $\sin/\cos$ functions of the mixing angles β and α, the continuum hh cross sections are suppressed compared to the Standard Model. The size of the cross sections increases for moderate $\tan\beta$ by nearly an order of magnitude if the hh final state can be generated in the chain $e^+e^- \to ZH \to Zhh$ via resonant H Higgs-strahlung. If the light Higgs mass approaches the upper limit for a given value of $\tan\beta$, the decoupling theorem drives the cross section of the supersymmetric Higgs boson back to its Standard Model value since the Higgs particles A, H, $H^\pm$ become asymptotically heavy in this limit. As a result of the decoupling theorem, resonance production is not effective for large $\tan\beta$. If the H mass is large enough to allow for decays to hh pairs, the ZZH coupling is already too small to generate a sizable cross section.

While the basic structure for the cross sections of the other ZH_iH_j [$H_{i,j} = h$, H] final states remains the same, the complexity increases due to unequal masses of the final-state particles. The double differential cross section of the process $e^+e^- \to ZH_iH_j$ is given for unpolarized beams by the expression

$$\frac{d\sigma[e^+e^- \to ZH_iH_j]}{dx_1 dx_2} = \frac{\sqrt{2}\, G_F^3\, M_Z^6}{384\,\pi^3 s} \frac{v_e^2 + a_e^2}{(1-\mu_Z)^2}\, \mathcal{Z}_{ij}(x_1, x_2) \tag{18}$$

The coefficients $\mathcal{Z}_{ij}$ in the cross sections can be written as

$$\begin{aligned} \mathcal{Z}_{ij} &= \mathfrak{z}_{ij}^2\, f_0 + \frac{\mathfrak{z}_{ij}}{2}\left[\frac{d_i d_j\, f_3}{y_1+\mu_{iZ}} + \frac{c_i c_j\, f_3}{y_1+\mu_{iA}}\right] + \frac{(d_i d_j)^2}{4\mu_Z(y_1+\mu_{iZ})}\left[\frac{f_1}{y_1+\mu_{iZ}} + \frac{f_2}{y_2+\mu_{jZ}}\right] \\ &+ \frac{(c_i c_j)^2}{4\mu_Z(y_1+\mu_{iA})}\left[\frac{f_1}{y_1+\mu_{iA}} + \frac{f_2}{y_2+\mu_{jA}}\right] + \frac{d_i d_j c_i c_j}{2\mu_Z(y_1+\mu_{iA})}\left[\frac{f_1}{y_1+\mu_{iZ}} + \frac{f_2}{y_2+\mu_{jZ}}\right] \\ &+ \Big\{(y_1,\mu_i) \leftrightarrow (y_2,\mu_j)\Big\} \end{aligned} \tag{19}$$

with

$$\mathfrak{z}_{ij} = \left[\frac{d_1 \lambda_{hH_iH_j}}{y_3-\mu_{1Z}} + \frac{d_2 \lambda_{HH_iH_j}}{y_3-\mu_{2Z}}\right] + \frac{2d_i d_j}{y_1+\mu_{iZ}} + \frac{2d_i d_j}{y_2+\mu_{jZ}} + \frac{\delta_{ij}}{\mu_Z} \tag{20}$$

The expressions for f_0 to f_3 have been denoted in Ref. [13]. The modifications of the SM Higgs-gauge coupling in the MSSM are accounted for by the mixing parameters:

$$\begin{array}{ll} VVh\text{:}\ d_1 = \sin(\beta-\alpha) & VVH\text{:}\ d_2 = \cos(\beta-\alpha) \\ VAh\text{:}\ c_1 = \cos(\beta-\alpha) & VAH\text{:}\ c_2 = -\sin(\beta-\alpha) \end{array} \tag{21}$$

for $V = Z$ and W. The reduction of the Zhh cross section is partly compensated by the ZHh and ZHH cross sections so that their sum adds up approximately to the SM value, if kinematically possible, as demonstrated in Fig. 6a for $\tan\beta = 3$ at $\sqrt{s} = 500$ GeV and hh, Hh and HH final states.

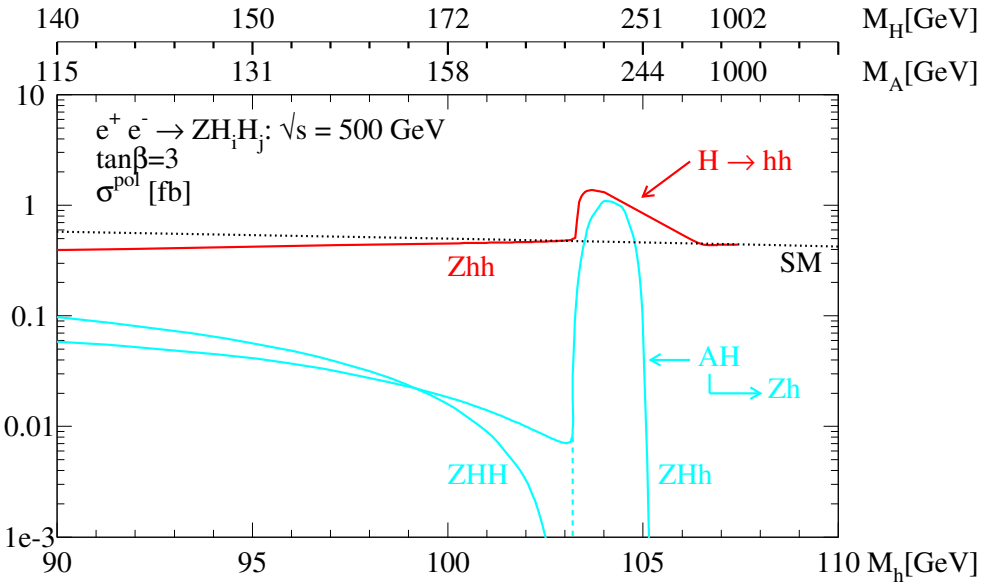

Figure 6a: *Cross sections for the processes Zhh, ZHh and ZHH for* $\sqrt{s} = 500$ *GeV and* $tan\beta = 3$, *including mixing effects* ($A = 1$ *TeV*, $\mu = -1$ *TeV*).

3.2 Triple-Higgs Production

The 2-particle processes $e^+e^- \to ZH_i$ and $e^+e^- \to AH_i$ are among themselves and mutually complementary to each other in the MSSM [29], coming with the coefficients $\sin^2(\beta-\alpha)/\cos^2(\beta-\alpha)$ and $\cos^2(\beta-\alpha)/\sin^2(\beta-\alpha)$ for $H_i = h, H$, respectively. Since multi-Higgs final states are mediated by virtual h, H bosons, the two types of self-complementarity and mutual complementarity are also operative in double-Higgs production: $e^+e^- \to ZH_iH_j$, ZAA and AH_iH_j, AAA. As the different mechanisms are intertwined, the complementarity between these 3-particle final states is of more complex matrix form, as evident from Fig. 3.

We will analyze in this section *in detail* the processes involving only the light neutral Higgs boson h, $e^+e^- \to Ahh$. The more cumbersome analyses for heavy neutral Higgs bosons H and other channels have been presented in Ref. [13].

In the first case one finds for the unpolarized cross section

$$\frac{d\sigma[e^+e^- \to Ahh]}{dx_1 dx_2} = \frac{G_F^3 M_Z^6}{768\sqrt{2}\pi^3 s} \frac{v_e^2 + a_e^2}{(1-\mu_Z)^2} \mathfrak{A}_{11}(x_1, x_2) \tag{22}$$

where the function $\mathfrak{A}_{11}$ reads

$$\begin{aligned} \mathfrak{A}_{11} &= \left[\frac{c_1\lambda_{hhh}}{y_3-\mu_{1A}} + \frac{c_2\lambda_{Hhh}}{y_3-\mu_{2A}}\right]^2 \frac{g_0}{2} + \frac{c_1^2\lambda_{hAA}^2}{(y_1+\mu_{1A})^2} g_1 + \frac{c_1^2 d_1^2}{(y_1+\mu_{1Z})^2} g_2 \\ &+ \left[\frac{c_1\lambda_{hhh}}{y_3-\mu_{1A}} + \frac{c_2\lambda_{Hhh}}{y_3-\mu_{2A}}\right] \left[\frac{c_1\lambda_{hAA}}{y_1+\mu_{1A}} g_3 + \frac{c_1 d_1}{y_1+\mu_{1Z}} g_4\right] + \frac{c_1^2\lambda_{hAA}^2}{2(y_1+\mu_{1A})(y_2+\mu_{1A})} g_5 \end{aligned}$$

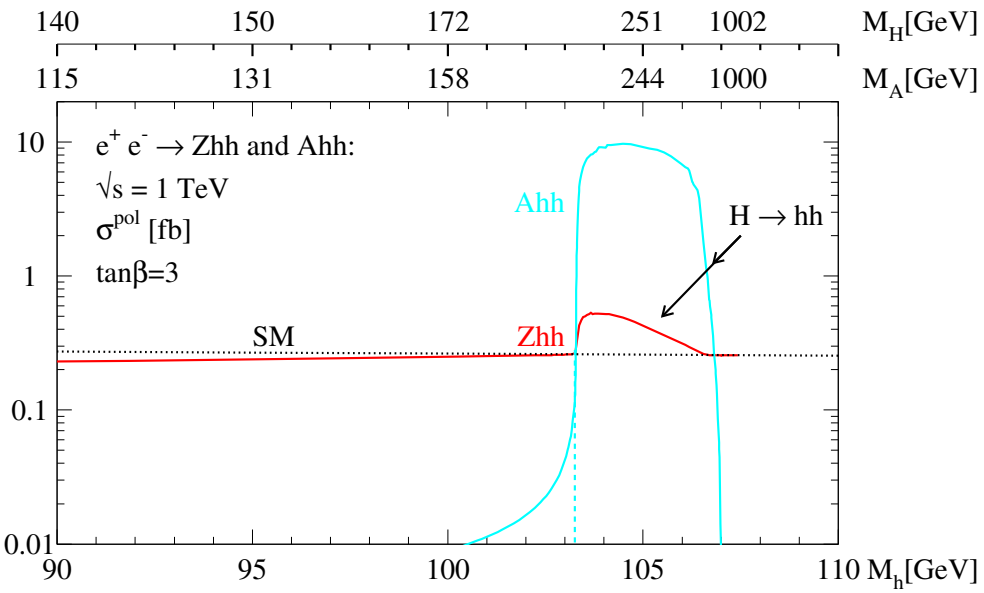

Figure 6b: *Cross sections of the processes Zhh and Ahh for* $\tan\beta = 3$ *and* $\sqrt{s} = 1$ *TeV, including mixing effects (*$A = 1$ *TeV,* $\mu = -1$ *TeV).*

$$
\begin{aligned}
&+ \quad \frac{c_1^2 d_1 \lambda_{hAA}}{(y_1+\mu_{1A})(y_1+\mu_{1Z})} g_6 + \frac{c_1^2 d_1 \lambda_{hAA}}{(y_1+\mu_{1A})(y_2+\mu_{1Z})} g_7 + \frac{c_1^2 d_1^2}{2(y_1+\mu_{1Z})(y_2+\mu_{1Z})} g_8 \\
&+ \quad \Big\{ y_1 \leftrightarrow y_2 \Big\}
\end{aligned}
\tag{23}
$$

with $\mu_{1,2} = M_{h,H}^2/s$. The coefficients g_k are listed in Ref. [13].

The general form of the double differential cross section of the process $e^+e^- \to AH_iH_j$ for unpolarized beams reads in the same notation as above:

$$
\frac{d\sigma[e^+e^- \to AH_iH_j]}{dx_1 dx_2} = \frac{G_F^3 M_Z^6}{768\sqrt{2}\pi^3 s} \frac{v_e^2 + a_e^2}{(1-\mu_Z)^2} \, \mathfrak{A}_{ij}(x_i, x_2) \tag{24}
$$

with the function $\mathfrak{A}_{ij}(x_1, x_2)$ defined by

$$
\begin{aligned}
\mathfrak{A}_{ij} \quad = \quad & \left[\frac{\lambda_{hH_iH_j} c_1}{y_3 - \mu_{1A}} + \frac{\lambda_{HH_iH_j} c_2}{y_3 - \mu_{2A}} \right]^2 g_0 + \frac{\lambda_{H_jAA}^2 c_i^2}{(y_1+\mu_{iA})^2} g_1 + \frac{\lambda_{H_iAA}^2 c_j^2}{(y_2+\mu_{jA})^2} g_1' \\
& + \frac{c_j^2 d_i^2}{(y_1+\mu_{iZ})^2} g_2 + \frac{c_i^2 d_j^2}{(y_2+\mu_{jZ})^2} g_2' + \left[\frac{\lambda_{hH_iH_j} c_1}{y_3 - \mu_{1A}} + \frac{\lambda_{HH_iH_j} c_2}{y_3 - \mu_{2A}} \right] \\
& \times \left[\frac{\lambda_{H_jAA} c_i}{y_1+\mu_{iA}} g_3 + \frac{\lambda_{H_iAA} c_j}{y_2+\mu_{jA}} g_3' + \frac{c_j d_i}{y_1+\mu_{iZ}} g_4 + \frac{c_i d_j}{y_2+\mu_{jZ}} g_4' \right] \\
& + \frac{\lambda_{H_iAA}\lambda_{H_jAA} c_i c_j}{(y_1+\mu_{iA})(y_2+\mu_{jA})} g_5 + \frac{c_i c_j d_i d_j}{(y_1+\mu_{iZ})(y_2+\mu_{jZ})} g_8 + \frac{\lambda_{H_jAA} c_i c_j d_i}{(y_1+\mu_{iA})(y_1+\mu_{iZ})} g_6 \\
& + \frac{\lambda_{H_iAA} c_i c_j d_j}{(y_2+\mu_{jA})(y_2+\mu_{jZ})} g_6' + \frac{\lambda_{H_jAA} c_i^2 d_j}{(y_1+\mu_{iA})(y_2+\mu_{jZ})} g_7 + \frac{\lambda_{H_iAA} c_j^2 d_i}{(y_2+\mu_{jA})(y_1+\mu_{iZ})} g_7'
\end{aligned}
\tag{25}
$$

The coefficients g_k were given in Ref. [13].

The size of the total cross section $\sigma[e^+e^- \to Ahh]$ is compared with double Higgs-strahlung $\sigma[e^+e^- \to Zhh]$ in Fig. 6b for $\tan\beta = 3$ at $\sqrt{s} = 1$ TeV. The cross section involving the pseudoscalar Higgs boson is small in the continuum. The effective coupling in the chain $Ah_{virt} \to Ahh$ is $\cos(\beta-\alpha)\lambda_{hhh}$ while in the chain $AH_{virt} \to Ahh$ it is $\sin(\beta-\alpha)\lambda_{Hhh}$; both products are small either in the first or in the second coefficient. Only for resonance H decays $AH \to Ahh$ the cross section becomes very large as expected from the decoupling theorem.

3.4 Sensitivity Areas

The results obtained in the preceding sections can be summarized in compact form by constructing sensitivity areas for the trilinear SUSY Higgs couplings based on the cross sections for double Higgs-strahlung and triple Higgs production. WW double-Higgs fusion can provide additional information on the Higgs self-couplings, in particluar for large collider energies.

The sensitivity areas will be defined in the [M_A, $\tan\beta$] plane [19]. The criteria for accepting a point in the plane as accessible for the measurement of a specific trilinear coupling are set as follows:

$$\begin{array}{ll} (i) & \sigma[\lambda] > 0.01 \text{ fb} \\ (ii) & \text{eff}\{\lambda \to 0\} > 2 \text{ st.dev.} \quad \text{for} \quad \int \mathcal{L} = 2 \text{ ab}^{-1} \end{array} \tag{26}$$

The first criterion demands at least 20 events in a sample collected for an integrated luminosity of 2 ab^{-1}, corresponding to the lifetime of a high-luminosity machine such as TESLA. The second criterion demands at least a 2 standard-deviation effect of the non-zero trilinear coupling away from zero. Even though the two criteria may look quite loose, the tightening of (i) and/or (ii) does not have a large impact on the size of the sensitivity areas in the [M_A, $\tan\beta$] plane, see Ref. [23]. The second criterion was defined in Ref. [13] slightly different by introducing the relative variation of the trilinear couplings with respect to the MSSM. [Due to an algorithmic error, the sensitivity areas in Ref. [13] had been overestimated.] For the sake of simplicity, mixing effects are neglected in the analysis.

Sensitivity areas of the trilinear couplings among the scalar Higgs bosons h, H in the correlation matrix Table 1, are depicted in Figs. 7a and 7b. If at most one heavy Higgs boson is present in the final state, the lower energy $\sqrt{s} = 500$ GeV is more preferable in the case of double Higgs-strahlung. HH final states in double Higgs-strahlung and triple Higgs production including A give rise to larger sensitivity areas at the high energy $\sqrt{s} = 1$ TeV. Apart from small regions in which interference effects play a major role, the magnitude of the sensitivity regions in the parameter $\tan\beta$ is readily explained by the magnitude of the

parameters $\lambda \sin(\beta - \alpha)$ and $\lambda \cos(\beta - \alpha)$, shown individually in Figs. 2a and 2b. For large M_A the sensitivity criteria cannot be met any more either as a result of phase space effects or due to the suppression of the H, A propagators for large masses. While the trilinear coupling of the light neutral CP-even Higgs boson is accessible in nearly the entire MSSM parameter space, the regions for the λ's involving heavy Higgs bosons are rather restricted.

Since neither experimental efficiencies nor background related cuts are considered in this paper, the areas shown in Figs. 7a and 7b must be interpreted as maximal envelopes. They are expected to shrink when experimental efficiencies are properly taken into account; more elaborate cuts on signal and backgrounds, however, may help reduce their impact.

4. Conclusions

In this report we have analyzed the production of Higgs boson pairs and triple Higgs final states at e^+e^- linear colliders up to energies of 1 TeV. They will allow the measurement of the fundamental trilinear Higgs self-couplings. The first theoretical steps into this area have been taken by calculating the production cross sections in the Standard Model for Higgs bosons in the intermediate mass range and for Higgs bosons in the minimal supersymmetric extension.

The cross sections in the Standard Model for double Higgs-strahlung and triple Higgs production are small so that high luminosities are needed to perform these experiments. Even though the e^+e^- cross sections are smaller than the corresponding pp cross sections, the strongly reduced number of background events renders the search for the Higgs-pair signal events, through $bbbb$ final states for instance, easier in the e^+e^- environment than in jetty LHC final states. For sufficiently high luminosities even the first phase of these colliders with an energy of 500 GeV will allow the experimental analysis of self-couplings for Higgs bosons in the intermediate mass range.

The extended Higgs spectrum in supersymmetric theories gives rise to a plethora of trilinear and quadrilinear couplings. The hhh coupling is generally quite different from the Standard Model. It can be measured in hh continuum production at e^+e^- linear colliders. Other couplings between heavy and light scalar Higgs bosons can be measured as well, though only in restricted areas of the $[M_A, \tan\beta]$ parameter space as illustrated in the set of Figs. 7a and 7b. The trilinear couplings including the pseudoscalar Higgs boson A are predicted to be small in the MSSM; future experimental analyses are therefore expected to give rise to upper bounds on these couplings if the MSSM is realized in Nature. For more general supersymmetric theories a model-independent analysis must be performed in triple Higgs channels.

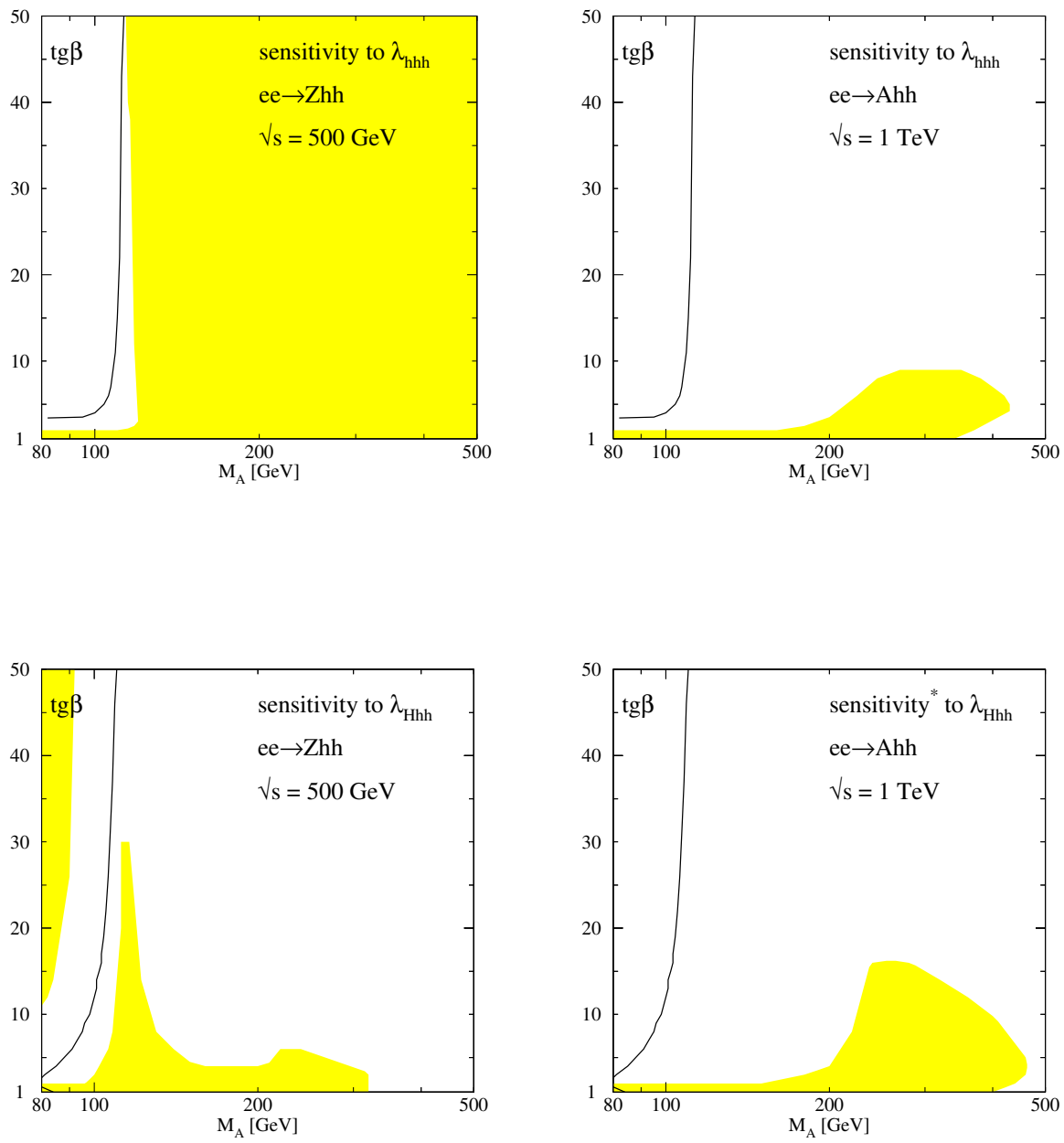

Figure 7a: *Sensitivity [* def = Ref.[13]] to the couplings λ_{hhh} and λ_{Hhh} in the processes $e^+e^- \to Zhh$ and $e^+e^- \to Ahh$ for collider energies 500 GeV and 1 TeV, respectively (no mixing). [Vanishing trilinear couplings are indicated by contour lines.]*

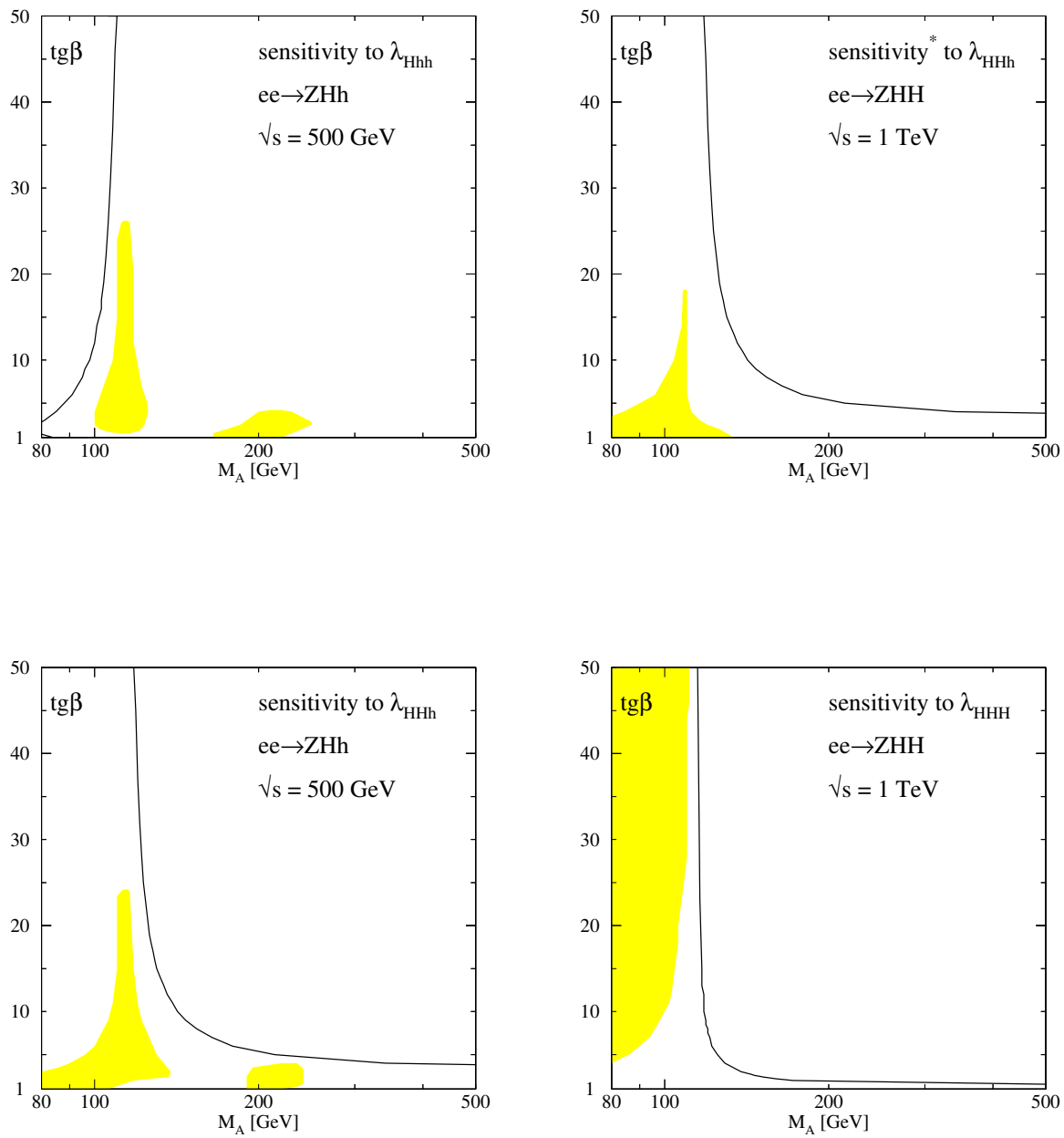

Figure 7b: *Sensitivity [* eff{$\lambda \to 0$} > 1st.dev.] to the couplings λ_{Hhh}, λ_{HHh} and λ_{HHH} in the processes $e^+e^- \to ZHh$ and $e^+e^- \to ZHH$ for collider energies 500 GeV and 1 TeV, respectively (no mixing).*

Acknowledgements

We gratefully acknowledge discussions with P. Gay, P. Lutz, L. Maiani, P. Osland and F. Richard.

References

[1] P.W. Higgs, Phys. Lett. **12** (1964) 132; and Phys. Rev. **145** (1966) 1156; F. Englert and R. Brout, Phys. Rev. Lett. **13** (1964) 321; G.S. Guralnik, C.R. Hagen and T.W. Kibble, Phys. Rev. Lett. **13** (1964) 585.

[2] For reviews see: J.F. Gunion, H.E. Haber, G. Kane and S. Dawson, *The Higgs Hunter's Guide*, Addison-Wesley, 1990; C. Quigg, XXVII Int. Meeting on Fundamental Physics, Sierra Nevada (Granada), [hep-ph/9905369]; M. Spira and P.M. Zerwas, Int. Universitätswochen, Schladming 1997, [hep-ph/9803257].

[3] G. Gounaris, D. Schildknecht and F. Renard, Phys. Lett. **B83** (1979) 191 and (E) **89B** (1980) 437; V. Barger, T. Han and R.J.N. Phillips, Phys. Rev. **D38** (1988) 2766.

[4] V.A. Ilyin, A.E. Pukhov, Y. Kurihara, Y. Shimizu and T. Kaneko, Phys. Rev. **D54** (1996) 6717.

[5] F. Boudjema and E. Chopin, Z. Phys. **C73** (1996) 85.

[6] V. Barger and T. Han, Mod. Phys. Lett. **A5** (1990) 667.

[7] A. Dobrovolskaya and V. Novikov, Z. Phys. **C52** (1991) 427.

[8] D.A. Dicus, K.J. Kallianpur and S.S.D. Willenbrock, Phys. Lett. **B200** (1988) 187; A. Abbasabadi, W.W. Repko, D.A. Dicus and R. Vega, Phys. Rev. **D38** (1988) 2770; Phys. Lett. **B213** (1988) 386.

[9] E.W.N. Glover and J.J. van der Bij, Nucl. Phys. **B309** (1988) 282.

[10] T. Plehn, M. Spira and P.M. Zerwas, Nucl. Phys. **B479** (1996) 46; (E) Nucl. Phys. **B531** (1998) 655.

[11] S. Dawson, S. Dittmaier and M. Spira, Phys. Rev. **D58** (1998) 115012.

[12] G. Jikia, Nucl. Phys. **B412** (1994) 57.

[13] A. Djouadi, W. Kilian, M. Mühlleitner, P.M. Zerwas, Eur. Phys. J. **C10** (1999) 27.

[14] P. Gay and P. Lutz, Talks at the ECFA/Desy LC Workshop, Obernai and Oxford 1999.

[15] D.J. Miller and S. Moretti, RAL preprint RAL-TR-1999-32 [hep-ph/9906395] and Eur. Phys. J. **C** *in press*.

[16] J.F. Gunion and H.E. Haber, Nucl. Phys. **B272** (1986) 1and **B278** (1986) 449.

[17] H.E. Haber and R. Hempfling, Phys. Rev. Lett. **66** (1991) 1815; Y. Okada, M. Yamaguchi and T. Yanagida, Prog. Theor. Phys. **85** (1991) 1; J. Ellis, G. Ridolfi and F. Zwirner, Phys. Lett. **B257** (1991) 83.

[18] M. Carena, J.R. Espinosa, M. Quiros and C.E.M. Wagner, Phys. Lett. **B335** (1995) 209; M. Carena, M. Quiros and C.E.M. Wagner, Nucl. Phys. **B461** (1996) 407; H.E. Haber, R. Hempfling and A.H. Hoang, Z. Phys. **C75** (1997) 539; S. Heinemeyer, W. Hollik and G. Weiglein, Eur. Phys. J. **C9** (1999) 343.

[19] A. Djouadi, H.E. Haber and P.M. Zerwas, Phys. Lett. **B375** (1996) 203.

[20] A. Djouadi, J. Kalinowski and M. Spira, Comput. Phys. Comm. **108** (1998) 56; M. Spira, *private communication*.

[21] M. Carena and P.M. Zerwas et al., Proceedings, *Physics at LEP2*, CERN 96-01 (1996) [hep-ph/9602250].

[22] A. Djouadi, J. Kalinowski and P.M. Zerwas, Z. Phys. **C70** (1996) 435.

[23] P. Osland and P.N. Pandita, Phys. Rev. **D59** (1999) 055013.

[24] M.N. Dubinin and A.V. Semenov, SNUTP-98-140 [hep-ph/9812246].

[25] A. Djouadi, W. Kilian, M. Muhlleitner and P.M. Zerwas, Higgs pair-production at high-energy colliders, XXIX *Int. Conference on High Energy Physics*, Vancouver 1998, Heidelberg Report HD-THEP 98-29; W. Kilian and P.M. Zerwas, Proceedings, XXIX *Int. Conference on High Energy Physics*, Vancouver 1998, [hep-ph/9809486].

[26] A. Djouadi, W. Kilian, M. Mühlleitner, P.M. Zerwas, Eur. Phys. J. **C10** (1999) 45.

[27] E. Accomando et al., Phys. Rep. **299** (1998) 1.

[28] R. Brinkmann, TESLA Collaboration, ECFA/DESY LC Workshop, Orsay 1998.

[29] A. Djouadi, J. Kalinowski and P.M. Zerwas, Z. Phys. **C57** (1993) 569.